IEEE Photonics Journal
An IEEE Photonics Society Publication

Open Access

A Raman-Pumped Dispersion and Nonlinearity Compensating Fiber For Fiber Optic Communications

Volume 12, Number 1, February 2020

Elham Bidaki
Shiva Kumar, ***Member, IEEE***

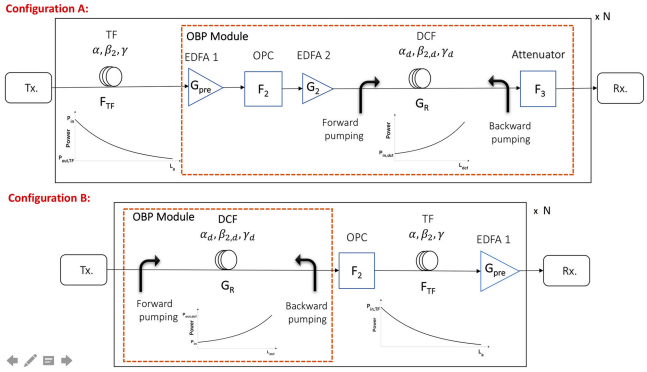

DOI: 10.1109/JPHOT.2019.2947213

A Raman-Pumped Dispersion and Nonlinearity Compensating Fiber For Fiber Optic Communications

Elham Bidaki and Shiva Kumar, *Member, IEEE*

Department of Electrical and Computer Engineering, McMaster University, Hamilton, ON L8S 4L8, Canada

DOI:10.1109/JPHOT.2019.2947213

Manuscript received July 18, 2019; revised September 30, 2019; accepted October 8, 2019. Date of publication October 14, 2019; date of current version January 7, 2020. Corresponding author: Elham Bidaki (e-mail: Bidakie@mcmaster.ca).

Abstract: An optical back propagation (OBP) technique using Raman pumped dispersion compensation fibers (DCF) is investigated to compensate for nonlinear impairments in WDM systems in real time. The proposed inline OBP module consists of an optical phase conjugator, amplifiers and a Raman pumped DCF. In order to suppress the nonlinear effects of the transmission fibers exactly, the power in the backpropagation fiber should increase exponentially with distance. This can be approximately achieved by using forward/backward Raman pumping of the dispersion compensating fiber (DCF). We introduce two configurations to realize the OBP. In this paper, we show that the OBP with forward/backward pumping provides 2.45 dB Q-factor gain compared to single-channel digital back propagation (DBP) when transmission distance is 1500 km for a WDM system with QAM-64. To minimize the variation of effective gain coefficient of the Raman pumped DCF as a function of distance, bidirectional pumping scheme which can provide the signal power profile closest to that required by the ideal OBP condition is proposed. The bidirectional pumping scheme provides a superior performance over forward/backward pumping and wideband DBP (i.e., DBP is applied on the entire WDM signal). Our numerical simulation results show that the bidirectional pumping scheme provides 7.6 dB and 5 dB advantage in Q-factor as compared to single-channel DBP and wideband DBP, respectively at a transmission distance of 5000 km. The maximum achievable reach of a long haul WDM system can be enhanced by 225% using bidirectional pumping scheme as compared to wideband DBP.

Index Terms: Nonlinear impairments, optical back propagation, raman amplification.

1. Introduction

The maximum reach of a fiber optic system is mainly limited by fiber nonlinear impairments which can be divided into two types: (i) deterministic (although symbol pattern dependent) nonlinear impairments that depend only on dispersion and nonlinearity such as self-phase modulation (SPM) [1], intra-channel cross-phase modulation (IXPM) and four wave mixing (IFWM) [2]–[4], and inter-channel cross-phase modulation (XPM) and four wave mixing (FWM) [1], [5], [6] (ii) stochastic nonlinear impairments that depend on the interplay between nonlinearity, amplified spontaneous emission (ASE) and dispersion [7]–[9]. The compensation of these impairments can be divided into three types: (i) digital [10]–[23], (ii) optical [24]–[32] and (iii) optoelectronic [33], [34]. In digital back propagation (DBP), virtual fibers with negative dispersion, loss and nonlinear coefficients are realized in digital domain [10]–[14]. Although the DBP can compensate for deterministic nonlinear impairments, it cannot compensate for stochastic nonlinear impairments. Besides, it is currently

limited to compensate for intra-channel nonlinear distortions only since in an optical network, a receiver does not have access to other channels that are dropped at other nodes [31]. In principle, the DBP can be used to compensate for inter-channel nonlinear distortion in a WDM point-to-point system [13]. However, it has not been implemented in real time due to limitations on computational resources and challenges to combine the outputs of many coherent receivers. In contrast, optical back propagation (OBP) can compensate for both intra-channel and inter-channel nonlinear impairments of a WDM system in real time [30]–[32]. In OBP, virtual fibers of DBP are replaced by real fibers/photonic devices. Since fibers with negative nonlinear coefficients do not exist, the optical phase conjugation (OPC) is used. An advantage of OBP technique is that it can partially compensate for stochastic nonlinear impairments if inline OBP is used [31]. However, there are a few hurdles to realize OBP in practical systems. First, photonic devices of OBP introduce losses and to compensate for losses, amplifier gain has to be increased leading to reduction in optical signal-to-noise ratio (OSNR). Second, in Refs. [30]–[32] dispersion-decreasing fiber (DDF)/dispersion-varying fiber (DVF) is proposed to realize ideal OBP. Although DDF-/DVF-based OBP provides significant performance improvement, the fabrication of DDF/DVF is difficult since dispersion of such fibers should vary as a function of propagation distance. In this paper, we propose a Raman amplified dispersion and nonlinearity compensating fiber to compensate for dispersion and nonlinearity of the transmission fiber. Unlike the DDF/DVF of Refs. [30]–[32], the dispersion of the proposed fiber does not change as a function of its length; in fact, the commercially available dispersion compensating fiber (DCF) can be used for this purpose. The required signal power profile to mitigate the transmission fiber nonlinearity is achieved by adjusting the Raman pump power. We introduce two configurations. In configuration A, an inline OPC is used after the transmission fiber (TF), which is followed by a Raman-pumped DCF. As a result, the signal power in the DCF increases nearly exponentially with distance. To enhance the optical signal-to-noise ratio (OSNR), a second configuration is proposed in which the Raman-pumped DCF is placed as the first span followed by an OPC and the TF. The configuration B requires a fewer photonic devices and outperforms configuration A slightly. We also compare three types of pumping schemes: (i) forward, (ii) backward, and (iii) bidirectional. In the case of forward/backward pumping, the OBP scheme does not provide the exact nonlinearity compensation since the signal power evolution in the DCF deviates from the requirement of ideal OBP condition. This scheme provides a moderate performance improvement ($\approx$2.45 dB) as compared to single-channel DBP at a transmission distance of 1500 km. However, when the bidirectional pumping is used, we found that the signal power evolution in the DCF is nearly the same as that required by ideal OBP condition. Our results show that the OBP scheme based on bidirectional pumping outperforms that based on forward/backward pumping by 6.8 dB in Q-factor when the reach is 5000 km. We also find that this bidirectional pumping OBP scheme outperforms single-channel DBP and wideband DBP by 7.7 dB and 5 dB in Q-factor, respectively. The superior performance of the proposed scheme over DBP is due to the fact that it partially compensates for stochastic nonlinear impairments as well. It is well-known that midpoint OPC can mitigate fiber dispersion and nonlinear impairments [24], [25] and it has been demonstrated experimentally [26], [29]. We note that the proposed scheme differs from midpoint OPC for the following reason. In midpoint OPC systems, the transmission fibers after the OPC mitigates the dispersion and nonlinearity effects of the fibers preceding the OPC, if there is a power symmetry about the point of phase conjugation. Although the midpoint OPC can provide significant performance improvement in point-to-point systems such as transoceanic systems, the performance improvement is marginal in optical networks due to the fact that amplifier spacings in North America vary from 50 km to 150 km randomly. As a result, the fibers following the OPC cannot mitigate the nonlinear effects of the fibers preceding the OPC exactly. Hence, there is a need to introduce a dedicated photonic device at each node (or inline) to compensate for the nonlinear impairments of the transmission fiber. The Raman amplified DCF proposed in this paper achieves this goal and the parameters of this sub-system can be tuned to achieve the desired nonlinearity compensation for the transmission fiber of arbitrary lengths.

Raman amplification in DCF has drawn significant attention in the past [35]–[38] owing to the fact that Raman gain efficiency of DCF is 7 to 10 times higher than standard single-mode fiber (SSMF). The Raman pumped DCF acts as an ampifier as well as the dispersion compensator [38].

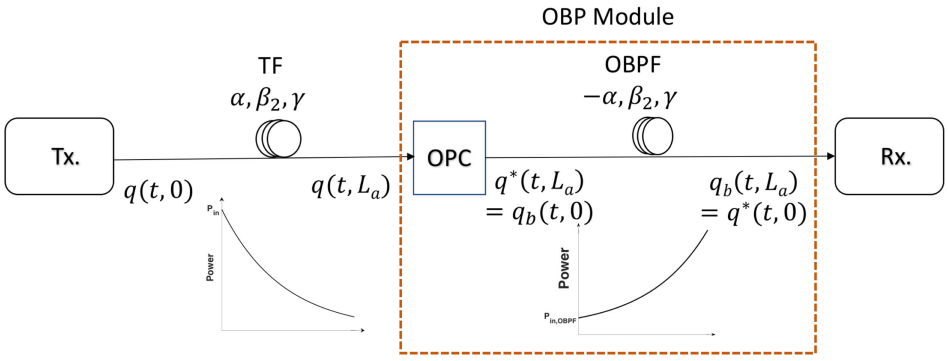

Fig. 1. A single-span fiber optic system with OBP using an ideal optical backpropagation fiber with negative loss coefficient. Tx: transmitter; TF: transmission fiber; OPC: optical phase conjugator; OBPF: optical backpropagation fiber; Rx: receiver.

The proposed Raman pumped DCF may be interpreted as an amplifier and compensator for both dispersion and nonlinearity.

The rest of the paper is organized as follows. In Section 2, conditions for ideal OBP are derived and Section 3 disscuses how to satisfy the OBP conditions using the Raman pumped DCF. The optimal pump ratio for the bidirectional pumping is calculated. Section 4 provides two system configurations and in Section 5, numerical simulation of these configurations for various pumping schemes is carried out. The Q-factor of the of the proposed schemes are compared with single-channel DBP and wideband DBP. The summery of the paper is provided in Section 6.

2. OBP Theory

2.1 Ideal Optical Back Propagation

Consider a single span of a transmission fiber (TF) of length L_a. The propagation of the field envelope in a fiber in the absence of noise is described by the nonlinear Schrödinger equation (NLSE):

$$\frac{dq}{dz} = i[D(t) + N(t,z)]q(t,z), \tag{1}$$

where

$$D(t) = -\frac{\beta_2}{2}\frac{\partial^2}{\partial t^2} + i\frac{\alpha}{2}, \tag{2}$$

$$N(t,z) = \gamma|q(t,z)|^2. \tag{3}$$

D and N denote the linear and nonlinear operators, respectively. Here, β_2, α and γ represent dispersion, loss and nonlinear coefficients, respectively. The formal solution of Eq. (1) is

$$q(t,L_a) = M\,q(t,0), \tag{4}$$

where M is the propagation operator,

$$M = e^{i\int_0^{L_a}[D(t)+N(t,s)]ds}. \tag{5}$$

Suppose the output signal of the transmission fiber which is described by Eq. (4) passes through an optical phase conjugator (OPC) (see Fig. 1). The conjugated signal becomes

$$q^*(t,L_a) = e^{-i\int_0^{L_a}[D^*(t)+N(t,z)]dz}q^*(t,0) = M^*q^*(t,0). \tag{6}$$

Let the conjugated signal propagate through an OBP fiber (OBPF) with a propagation operator M'. The purpose of OBPF is to compensate exactly for dispersive and nonlinear distortions caused by

the TF. The output of OBPF,

$$q_b(t, L_a) = M' q^*(t, L_a), \tag{7}$$

is identical to the conjugated input signal $q^*(t, 0)$ only if $M'M^* = I$ where I is the identity operator. Hence,

$$M' = (M^*)^{-1} = e^{j\int_0^{L_a}[D^*(t)+N(t,s)]ds}, \tag{8}$$

where

$$D^*(t) = -\frac{\beta_2}{2}\frac{\partial^2}{\partial t^2} - i\frac{\alpha}{2}. \tag{9}$$

Thus, the OBP fiber is identical to the transmission fiber except its loss coefficient is $-\alpha$. The input field envelope can be retrieved by taking the complex conjugate of the received signal in the electrical domain at the receiver. Eq. (7) with the propagation operator of M' given by Eq. (8) is equivalent to

$$\frac{\partial q_b}{\partial z_b} = i[D^*(t) + N(t, z_b)]q_b(t, z_b), \tag{10}$$

with $q_b(t, 0) = q^*(t, L_a)$ and z_b is the distance in OBPF. Eq. (10) describes the evolution of the optical signal in OBPF. Let

$$q_b(t, z_b) = \sqrt{P_{in,OBPF}}\, e^{\frac{\alpha z_b}{2}} u_b(t, z_b), \tag{11}$$

where $P_{in,OBPF}$ is the power launched to OBPF,

$$P_{in,OBPF} = P_{in} e^{-\alpha L_a}, \tag{12}$$

and P_{in} is the launch power to the TF. The reason for the exponential function in Eq. (11) is that the signal power in the OBP fiber increases exponentially with distance. Also, for later convenience, we use the following transformation

$$dz_b' = \beta_2 dz_b. \tag{13}$$

Using Eqs. (11) and (13), Eq. (10) may be rewritten as

$$i\frac{\partial u_b}{\partial z_b'} - \frac{1}{2}\frac{\partial^2 u_b}{\partial t^2} + \frac{\gamma P_{in}}{\beta_2} e^{-\alpha(L_a - z_b)}|u_b|^2 u_b = 0. \tag{14}$$

Eq. (14) describes the field propagation in an ideal fiber with a negative loss coefficient α (or equivalently the power increasing with distance) which exactly compensates for dispersion and nonlinearity of the TF.

We note that this ideal fiber (OBPF) with negative loss coefficient does not exist. In Ref. [30], the characteristics of the ideal fiber is realized using a DDF. In this paper, we investigate the possibility of realizing it using a dispersion compensation fiber (DCF) with distributed Raman amplification.

2.2 Ideal OBP Using Distributed Amplification

To derive an equivalent way of realizing the ideal back propagation equation (Eq. (14)), let the output signal of the OPC, $q_b(t, 0) = q^*(t, L_a)$, propagate through a DCF whose effective loss profile is a function of distance $\alpha_d(z_d)$, where z_d is the distance in DCF (see Fig. 2).

Using transformations

$$q(z_d, t) = \sqrt{P_{in,d}}\, e^{-\frac{1}{2}\int_0^{z_d}\alpha_d(z')dz'} u_b, \tag{15}$$

and

$$dz_d' = \beta_{2,d} dz_d, \tag{16}$$

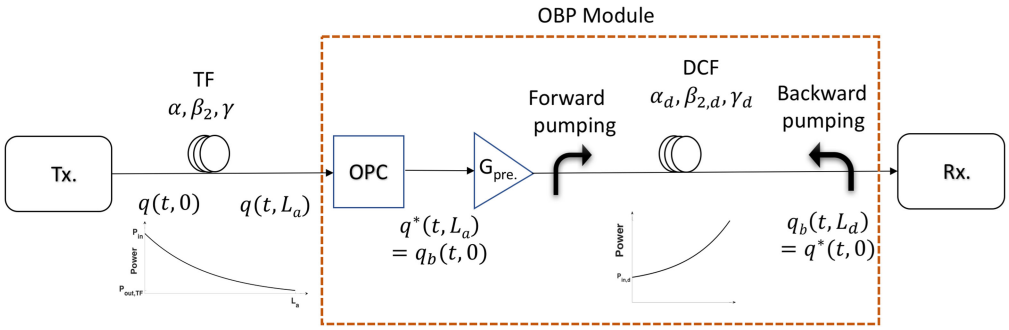

Fig. 2. A single-span fiber optic system with OBP using a Raman pumped DCF and amplifiers. Tx: transmitter; TF: transmission fiber; OPC: optical phase conjugator; OBPF: optical backpropagation fiber; Rx: receiver.

Eq. (1) that describes the optical field envelope in this fiber can be rewritten as

$$i\frac{\partial u_b}{\partial z_d'} - \frac{1}{2}\frac{\partial^2 u_b}{\partial t^2} + \frac{\gamma_d P_{in,d}}{\beta_{2,d}} e^{-\int_0^{z_d} \alpha_d(z')dz'} |u_b|^2 u_b = 0, \tag{17}$$

where $\beta_{2,d}$ and γ_d are the dispersion and nonlinear coefficients of the DCF, respectively, and $P_{in,d}$ is the launch power to the DCF.

Eqs. (17) and (14) are identical only if

$$dz_b' = dz_d', \tag{18}$$

and

$$\frac{\gamma P_{in}}{\beta_2} e^{-\alpha(L_a - z_b)} = \frac{\gamma_d P_{in,d}}{\beta_{2,d}} e^{-\int_0^{z_d} \alpha_d(z')dz'}. \tag{19}$$

Substituting Eqs. (16) and (13) in Eq. (18), we obtain

$$\frac{dz_d}{dz_b} = \frac{\beta_2}{\beta_{2,d}}, \tag{20}$$

$$z_d = \frac{\beta_2}{\beta_{2,d}} z_b + c, \tag{21}$$

where c is a constant. Putting $z_d = 0$ when $z_b = 0$ yields $c = 0$.

Integrating Eq. (21), we find the length of the DCF as

$$L_d = \frac{\beta_2}{\beta_{2,d}} L_a. \tag{22}$$

It may be noted that the length of the ideal OBPF is the same as that of the TF (i.e., L_a) whereas the length of the DCF (i,e., L_d) could be much smaller if $|\beta_{2,d}| \gg |\beta_2|$.

Next, the constraints of Eq. (19) may be broken down into the following two constraints,

$$e^{\alpha z_b} = e^{-\int_0^{z_d} \alpha_d(z')dz'}, \tag{23}$$

$$P_{in,d} = \frac{\gamma}{\gamma_d}\frac{\beta_{2,d}}{\beta_2} P_{in} e^{-\alpha L_a}. \tag{24}$$

From Eq. (24), we see that if $\beta_{2,d} = \beta_2$ and $\gamma_d = \gamma$, the launch power to the DCF is simply the output of the TF.

Eq. (23) can be satisfied only if α_d is constant, i.e.,

$$\alpha z_b = -\alpha_d z_d. \tag{25}$$

Using Eq. (21), we obtain an expression for the effective loss coefficient of DCF to have the ideal OBP as

$$\alpha_d = -\alpha \frac{\beta_{2,d}}{\beta_2}. \tag{26}$$

In Section 3, we discuss how to realize the effective loss/ gain coefficient α_d of DCF for various pumping configurations. For simplicity, we have based our analysis on the scalar nonlinear Schrödinger equation (NLSE). However, the results are also applicable for the case of dual polarization when the polarization mode dispersion (PMD) is ignored. In fact, our simulations in Section 5 consider dual polarizations.

3. Raman Pumping

3.1 Forward Raman Pumping

The evolution of the signal and pump powers in the DCF for the forward pumping scheme is governed by [1], [6]

$$\frac{dP_s}{dz_d} = \frac{g_R P_p P_s}{A_p} - \alpha_s P_s, \tag{27}$$

$$\frac{dP_p}{dz_d} = -\frac{\omega_p}{\omega_s}\frac{g_R P_p P_s}{A_s} - \alpha_p P_p, \tag{28}$$

where g_R is the Raman gain coefficient; P, A, α and ω denote the power, effective cross-section, loss coefficient and angular frequency, respectively, and the subscripts p and s denote the pump and the signal, respectively. If the depletion of the pump due to the transfer of power to the signal (first term on the right hand side of Eq. (28)) is ignored, the solution of Eq. (28) under this approximation is

$$P_p(z_d) = P_p^+(0) e^{-\alpha_p z_d}, \tag{29}$$

where $P_p^+(0)$ is the input pump power. Substituting Eq. (29) in Eq. (27) and solving for P_s, we find [1], [6]

$$P_s(z_d) = P_s(0) \exp\left[-\alpha_s z_d + \frac{g_R P_p^+(0)}{A_p} z_{eff}^+\right], \tag{30}$$

where

$$z_{eff}^+(z_d) = \frac{1 - \exp(-\alpha_p z_d)}{\alpha_p}. \tag{31}$$

Eq. (30) may be rewritten as

$$P_s(z_d) = P_s(0) \exp[-g_{eff}(z_d) z_d], \tag{32}$$

where

$$g_{eff}(z_d) = \alpha_s - \frac{g_R P_p^+(0)}{A_p} \frac{z_{eff}^+}{z_d}. \tag{33}$$

At $z_d = L_d$, the effective gain coefficient is

$$g_{eff}(L_d) = \alpha_s - \frac{g_R P_p^+(0)}{A_p} \frac{L_{eff}}{L_d}, \tag{34}$$

where $L_{eff} = z_{eff}^+(L_d)$. When $z_b = L_a$, $z_d = L_d$ and from Eq. (23), we find that one of the requirements for the ideal OBP is

$$e^{\alpha L_a} = e^{-g_{eff}(L_d) L_d}. \tag{35}$$

Simplifying Eq. (35), we find an expression for the input pump power as

$$P_{p0}^{+} \equiv P_{p}^{+}(0) = (\alpha L_a + \alpha_s L_d)\frac{A_p}{g_R L_{eff}}. \tag{36}$$

Taylor expansion of Eq. (31) yeilds

$$z_{eff}^{+} = z_d - \frac{\alpha_p z_d^2}{2!} + \frac{\alpha_p^2 z_d^3}{3!} + \cdots. \tag{37}$$

If $\alpha_p z_d \ll 1$, we find $z_{eff}^{+} \approx z_d$. Under this approximation, we have

$$g_{eff}(z_d) \approx \alpha_s - \frac{g_R P_{p0}^{+}}{A_p}. \tag{38}$$

Eq. (26) provides the effective loss coefficient required for the ideal OBP. Hence, equating Eqs. (38) and (26), we obtain

$$g_{eff} = -\frac{\alpha\beta_{2,d}}{\beta_2}. \tag{39}$$

If $\alpha_p L_d \ll 1$, the variation of g_{eff} as a function of z_d is very small and the ideal OBP condition of Eq. (39) can be approximately realized. So, to make this approximation more accurate, we would like to keep the length of DCF, L_d small. If we choose the DCF that has larger $|\beta_{2,d}|$ as compared to that of the TF, the required length L_d becomes smaller (see Eq. (22)).

In our simulations (see Section 5), we have used $L_d = 3.077$ km and for such a short length, we found that the signal power evolution given by Eq. (30) obtained by the pump undepletion approximation is reasonably accurate. We have solved the nonlinear coupled equations (27) and (28) numerically, and found that the maxmimum discrepancy between the signal power obtained by the numerical solution and Eq. (30) is $\approx$0.18 dB.

Due to the difference in dispersion and nonlinear coefficients between TF and DCF, the launch power to the DCF should be adjusted in accordance with Eq. (24). So, we introduce a pre-amplifier with gain G_{pre} (see Fig. 2) which can be adjusted so that the one of the OBP conditions (Eq. (24)) is satisfied.

3.2 Backward Raman Pump

Under the undepleted pump approximation, the evolution of the signal and pump powers in the DCF are given by [1]

$$P_p(z_d) = P_{p0}^{-}\exp\left[-\alpha_p(L_d - z_d)\right], \tag{40}$$

$$P_s(z_d) = P_{s0}\exp\left[-\alpha_s z_d + \frac{g_R P_{p0}^{-} e^{-\alpha_p L_d}}{Ap} z_{eff}^{-}\right], \tag{41}$$

$$z_{eff}^{-}(z_d) = \frac{e^{\alpha_p z_d} - 1}{\alpha_p}, \tag{42}$$

where P_{s0} is the signal power at $z_d = 0$ and P_{p0}^{-} is the pump power injected at $z_d = L_d$. Proceeding as before, the required pump power P_{p0}^{-} is found to the be same as that for forward pumping case (see Eq. (36)). If $\alpha_p z_d \ll 1$, $z_{eff}^{-} \approx z_d$ and in this case the effective gain coefficient becomes constant as required by the ideal OBP condition (Eq. (26)).

3.3 Bidirectional Pumping

We assume that there are two pumps, one co-propagating with the signal and the other counter-propagating (see Fig. 2). Under undepleted pump approximation, the evolution of signal is given

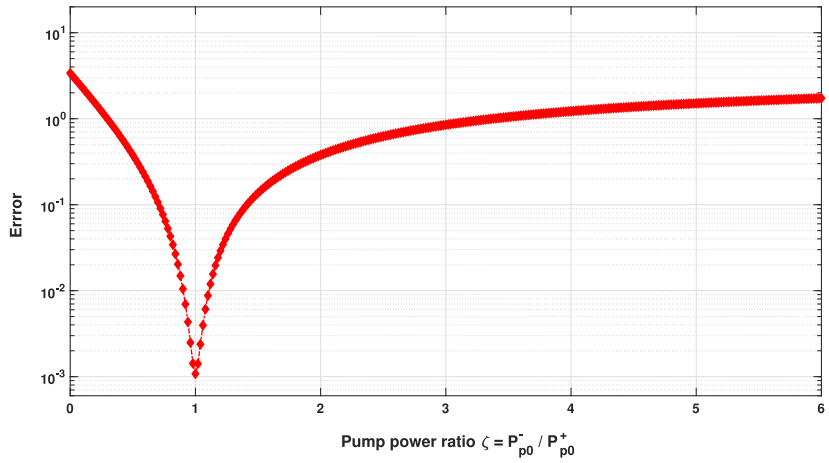

Fig. 3. Deviation of the power profile from the ideal power profile as a function the pump power ratio.

by

$$P_s(z_d) = P_{s0} \exp\left[-\alpha_s z_d + \frac{g_R}{A_p}(P_{p0}^{+} z_{eff}^{+} + P_{p0}^{-} e^{-\alpha_p L_d} z_{eff}^{-})\right], \tag{43}$$

where $P_{p0}^{+} = P_p^{+}(0)$ is the input power of the co-propagating pump and $P_{p0}^{-} = P_p^{-}(L_d)$ is the input power of the counter-propagating pump.

Using Eqs. (23), (25), (31) and (42), one of the requirements for the ideal OBP is

$$e^{\alpha L_a} = e^{-\alpha_s L_d + g_R L_{eff}(P_{p0}^{+} + P_{p0}^{-})/A_p}, \tag{44}$$

where $L_{eff} = \frac{1-\exp(-\alpha_p L_d)}{\alpha_p}$. Simplifying Eq. (44), we obtain

$$P_{p0} \equiv P_{p0}^{+} + P_{p0}^{-} = (\alpha L_a + \alpha_s L_d)\frac{A_p}{g_R L_{eff}}, \tag{45}$$

where P_{P0} is the total input pump power. Comparing Eqs. (36) and (45), we find that the sum of the input pump powers is the same as the input pump power of the case of the forward (or backward) pumping only.

Let the ratio of the input backward and forward pump powers be ζ, i.e., $\zeta = \frac{P_{p0}^{-}}{P_{p0}^{+}}$. Since the total input pump power P_{p0} is fixed (it should satisfy Eq. (45)), we have only one degree of freedom in the design of bidirectional pumping scheme, namely, the pump power ratio, ζ, which is optimum if the deviation of signal power profile from the ideal case (as required by the ideal OBP conditions, Eqs. (25) and (26)) is minimized. So, we consider the following optimization problem,

$$\underset{\zeta}{\text{minimize}} \quad e(\zeta)$$

where the error e is

$$e(\zeta) = \int_o^{L_d} |P_s^{ideal}(z_d) - P_s(z_d)| dz_d \quad \zeta = \frac{P_{p0}^{-}}{P_{p0}^{+}},$$

$P_s(z_d)$ is given by Eq. (43) and

$$P_s^{ideal}(z_d) = P_s(0) \exp\left(\frac{\alpha\beta_{2,d}}{\beta_2} z_d\right). \tag{46}$$

Fig. 3 shows the error as a function of ζ. As can be seen, the error i.e., the deviation of the actual power profile from the ideal power profile is minimum when the input forward and backward pump

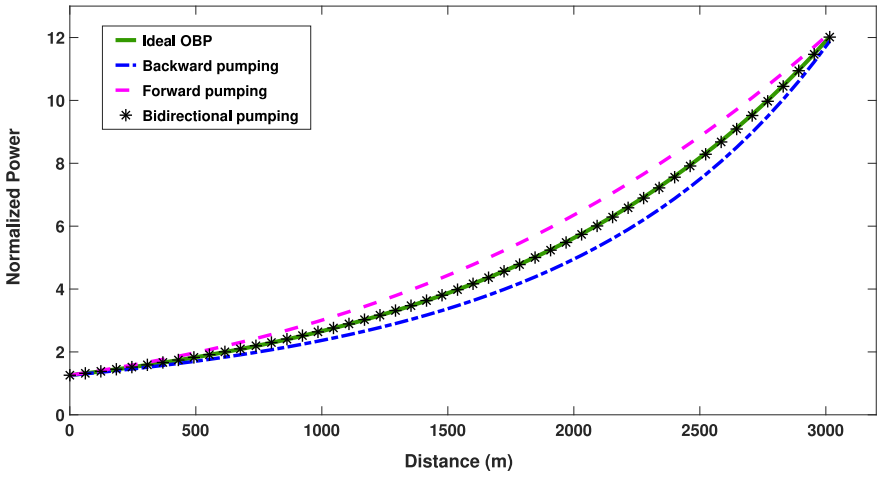

Fig. 4. Normalized power profile of the signal along the DCF. For bidirectional pumping, $\zeta = 1$. Length of the DCF = 3.077 km.

powers are equal ($\zeta = 1$). Fig. 4 shows the normalized signal power profile for forward/backward pumping only and bidirectional pumping cases. In the case of bidirectional pumping, we assume that the pump power ratio, ζ to be unity. As the length of the DCF is short, signal power profiles are close to exponential profiles. However, for the longer length of a Raman pumped fiber (e.g., $L_d = 50$ km), for example, using the forward pumping scheme, signal power increases nearly exponentially at the beginning and then starts decreasing due to the signal loss and pump depletion. Fig. 4 also shows the evolution of the signal power corresponding to the ideal case as required by OBP condition (Eq. (26)). As can be seen, in the case of forward power pumping, the power in the DCF exceeds that required by the ideal OBP whereas in the case of backward pumping, it is lower than that required by the ideal OBP. When bidirectional pumping with an optimum power ratio $\zeta = 1$ is used, the power profile is closest to that required by the ideal OBP.

When $\zeta = 1$, Eq. (43) may be written as

$$P_s(z_d) = P_{s0} \exp\left[-\alpha_s z_d + \frac{g_R P_p(0)}{A_p} z_{eff}\right], \tag{47}$$

where

$$z_{eff} = \frac{1}{2}\left(\frac{1 - e^{-\alpha_p z_d}}{\alpha_p} + \frac{e^{-\alpha_p (L_d - z_d)} - e^{-\alpha_p L_d}}{\alpha_p}\right). \tag{48}$$

Next, we show that the second order term in z_d in the expansion of the z_{eff} can be made significantly smaller using bidirectional pumping with $\zeta = 1$ so that z_{eff} is nearly equal to z_d, which is the requirement for the ideal OBP. Expanding exponential functions in Eq. (48) using Taylor series yields

$$\begin{aligned} z_{eff} = &\left(1 - \frac{x}{2} + \frac{x^2}{4} - \frac{x^3}{12} + \cdots\right) z_d \\ &+ \left(-\frac{x}{4} + \frac{x^2}{8} - \frac{x^3}{24} + \cdots\right) \alpha_p z_d^2 \\ &+ \left(\frac{1}{6} - \frac{x}{12} + \frac{x^2}{24} + \cdots\right) \alpha_p^2 z_d^3, \end{aligned} \tag{49}$$

where $x = \alpha_p L_d$. For example, when $\alpha_p = 0.138\ \text{km}^{-1}$, $L_d = 3.077$ km and $x = 0.425$. The coefficient of $\alpha_p z_d^2$ in Eq. (49) is -0.087 whereas it is -0.5 for the case of of the forward pumping (see Eq.

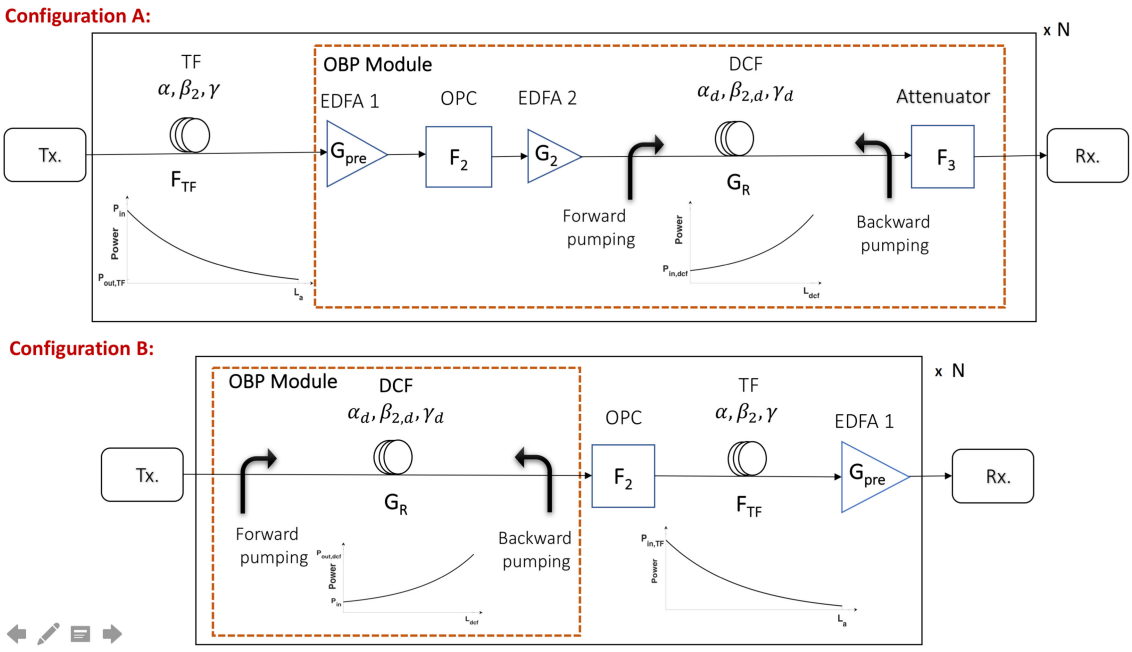

Fig. 5. Configuration A and B: N-span fiber optic system with OBP using a Raman pumped DCF and amplifiers. Tx: transmitter; TF: transmission fiber; OPC: optical phase conjugator; DCF: dispersion compensation fiber; Rx: receiver.

(37)). Thus, theres is a 82% reduction in the second order term in z_d using the bidirectional pumping. Hence, we expect that the OBP with bidirectional pumping shows better performance. In the Section 5, we find that the transmission performance improvement brought by OBP depends mainly on how close the signal power profile is to the ideal profile.

Ref. [39] uses bidirectional Raman pumps for 400 Gb/s PM-16QAM transmission over 1504 km over Verizon network fiber deployed around Dallas. The backward Raman module consists of pump wavelengths in the range of 1420 nm to 1500 nm and the forward Raman module includes 3 pump wavelengths (1420 nm–1480 nm). Multiple pump wavelengths are used for the purpose of gain flattening. Ref. [40] describes the bidirectional distributed Raman amplification scheme for 83.32 km SSMF in which the backward Raman pump is at 1365 nm and the forward Raman pump module consists of two pumps at 1365 nm and 1455 nm which are combined with the signal using a WDM coupler. The pump at 1455 nm is obtained by backward pumping a separate 10 km SSMF with a 1365 nm pump. Ref. [41] implements the bidirectional Raman pumping scheme over 84 km NZDSF in a WDM-PON system. Both forward and backward Raman pump modules use two pump wavelengths 1450 nm and 1460 nm, and provide a gain of ≈20 dB.

Generally, WDM couplers are used for multiplexing the pumps and the signal at the fiber input and output ends, and isolators are placed at both ends. More details on the implementation of bidirectional pumping can be found in Refs. [39]–[41]

4. OBP Configurations

We consider two OBP configurations (see Fig. 5). In configuration A, the OBP module post-compensates the dispersive and nonlinear effects of the TF whereas in configuration B, the OBP module pre-compensates it. Eq. (24) may be written as

$$P_{in,d}(dBm) = P_{in,TF}(dBm) - F_{TF}(dB) + G_{pre}(dB), \tag{50}$$

where F_{TF} is the loss due to the TF and

$$G_{pre} = 10 \times \log_{10} \frac{\gamma}{\gamma_d} \frac{\beta_{2,d}}{\beta_2}. \tag{51}$$

From Eq. (50), we see that the launch power to the DCF, $P_{in,d}$ should be larger than the output of the TF. As a result, in configuration A, we need to amplify the output of the TF by G_{pre}. Besides, OPC introduces a loss around 8 dB [31]. So, we need an amplifier, EDFA 2 with gain G_2 to compensate for the OPC loss (F_2). In order to meet the requirement of the ideal OBP, the Raman pumped DCF should provide a gain that is equal to loss of the TF. So, we are forced to introduce an attenuator, F_3 to compensate for the gain of the pre-amplifier (EDFA 1). So, the additional amplification by EDFA 1 to satisfy the OBP condition and the subsequent attenuation to compensate for it, leads to degradation in optical signal-to-noise ratio (OSNR). This problem can be solved by using configuration B in which the Raman pumped DCF precedes the TF. The theory of OBP developed in Section 2 are applicable to this configuration as well.

Next, we consider the power evolution in configuration B. Since the loss due to the TF (F_{TF}) is equal in magnitude to the net gain provided by the Raman amplification (G_R), but opposite in sign, Eq. (50) may be rewritten as

$$\begin{aligned} P_{out,d}(dBm) &= P_{in,d}(dBm) + F_{TF}(dB) \\ &= P_{in,TF}(dBm) + G_{pre}(dB), \end{aligned} \tag{52}$$

where $P_{out,d}$ is the output of DCF. From Eq. (52), we see that the input of the TF should be lower than the output of DCF by G_{pre} (dB). This means that we need to introduce attenuation after the DCF. Since the OPC introduce a loss which is of the order of G_{pre} (dB), it acts as the required attenuation and thereby, eliminates the need for the pair of amplification and attenuation required in configuration A.

The OSNR in configuration A is calculated as follows:

$$OSNR = \frac{P_{in}}{\sum_{j=1}^{3} P_{N,j}}, \tag{53}$$

where P_{in} is the output power of transmitter,

$$P_{N,j} = N n_{sp,EDFA} G_R F_3 (G_j - 1) h f \Delta f, \quad j = 1, 2, \tag{54}$$

$n_{sp,EDFA}$ is the spontaneous factor of EDFA, G_1, G_2, G_R and F_3 are the gains of EDFA 1, EDFA 2, Raman amplification and the loss due to the attenuator, respectively, and $\Delta f = 12.49$ GHz.

$$P_{N,3} = N n_{sp,R} F_3 h f \Delta f \sum_{k=1}^{N_R} \left[(G_k - 1) \prod_{i=k+1}^{N_R} G_i \right], \tag{55}$$

where $n_{sp,R}$ is the spontaneous factor of Raman amplifier. We have modeled distributed Raman amplification as a superposition of N_R discrete tiny amplifiers with gain G_k (see Section 5). The OSNR in scheme B is also calculated as follows:

$$OSNR = \frac{P_{in}}{\sum_{j=1}^{2} P_{N,j}}, \tag{56}$$

where

$$P_{N,1} = N n_{sp,R} F_{TF} h f \Delta f \sum_{k=1}^{N_R} \left[(G_k - 1) \prod_{i=k+1}^{N_R} G_i \right], \tag{57}$$

and

$$P_{N,2} = N n_{sp,EDFA} (G_{pre} - 1) h f \Delta f. \tag{58}$$

For example, when transmitter output power, $P_{in} = -10$ dBm, OSNR after $N = 30$ spans is 19.1 dB and 22.8 dB for configuration A and configuration B, respectively. Therefore, we expect the configuration B to show better performance over configuration A in the linear regime. However, in nonlinear regime (higher launch power), we cannot conclude which which configuration works better. Hence, we perform the numerical simulation of various OBP schemes in the next section.

5. Simulation Results

A 5-channel dual-polarization (DP) WDM fiber optic system is simulated using the following parameters: channel spacing = 50 GHz, symbol rate per channel = 28 Gsymbols/s, modulation = 64 quadrature amplitude modulation (QAM). The raised cosine pulses with a roll-off factor 0.2 is used. Number of symbols/channel simulated is 4096 and the computational bandwidth = 560 GHz. The transmission fiber is Corning's Metrocor fiber whose dispersion, loss and nonlinear coefficients are $\beta_2 = 8$ ps^2/km, $\alpha = 0.2$ dB/km and $\gamma = 2.2$ W^{-1} km^{-1}, respectively. TF length, $L_a = 50$ km. For the DCF, $\beta_{2,d} = 130$ ps^2/km, loss coefficient at signal wavelength (1550 nm), $\alpha_s = 0.4$ dB/km, $\gamma_d = 4.86$ W^{-1}km^{-1}, and $L_d = 3.077$ km. For the proposed technique, it is required that dispersion coefficient of TF and DCF have the same sign. The commercially available DCFs have large normal dispersions and hence Corning's Metrocor fiber is used as a transmission fiber whose dispersion is normal. The proposed approach could be adapted to anomalous dispersion regime without any changes if DCFs with large anomalous dispersion coefficients are available. It may be possible to fabricate DCFs with large anomalous dispersion, but it was not attempted mainly because the standard single-mode fibers (SSMF) have anomalous dispersion in the C-band. It may also be possible to develop Silicon Photonics based nonlinear waveguides with very large anomalous dispersion which could be a substitute for the DCF in the proposed technique.

The pre-amplifier gain, $G_{pre} = 8.67$ dB. We assume the signal loss due to OPC is 8 dB. The OPC can be realized by four-wave mixing (FWM), stimulated Brillouin scattering (SBS) or stimulated Raman scattering (SRS). The OPC is typically realized using highly nonlinear fibers (HNLF) with one or two laser pumps. The nonlinear mixing of the signal and the pumps produces a four wave mixing sideband which is proportional to the signal conjugate. More details about the OPC modeling can be found in Ref. [31], in which the non-ideal effects are also considered. The noise figure of EDFA (i.e., inline amplifiers/pre-amplifiers) is 4.77 dB. For a Raman pump, loss coefficient at pump wavelength (1450 nm), $\alpha_p = 0.6$ dB/km, $g_R/A_p = 2.2$ W^{-1} km^{-1}, and spontaneous noise factor $n_{sp,R} = 1.1$. Total input Raman pump power, $P_{p0} = 26.7$ dBm which is fixed for all three pumping schemes. The pumps have a RIN of -155 dB/Hz [42]. The DCF is divided into $N_R = 2000$ segments, which corresponds to a step size of 1.5 m. The Raman gain over a segment is determined by Eqs. (30), (41) and (43) for forward, backward and bidirectional, respectively. A tiny discrete amplifier is introduced at the end of the segment k with ASE power spectral density given by $\rho_{ASE,R} = n_{sp,R} hf(G_k - 1)$, where G_k is the gain of the kth discrete amplifier. As a sanity check, we changed the step size to 1 m and 0.5 m, and found that the BER remains constant. Fig. 6 shows the gain of the tiny amplifiers, G_k as a function of the DCF length. As can be seen, the gain is nearly constant as a function of length for the bidirectional scheme (as required by the OBP condition, Eq. (26)). This can be qualitatively understood as follows. For the case of forward pumping, the gain is higher at the beginning ($z_d \approxeq 0$) and it decreases at larger distance due to pump attenuation. In contrast, for backward pumping, the gain is higher near the end ($z_d \approxeq L_d$). When bidirectional pumping is used, the gain becomes nearly equal throughout the length of DCF. Total gain provided by the Raman amplifier is 11.23 dB.

We do not intend to make a rigorous modeling of Raman amplifier taking into account the effects such as reflection and single/double Rayleigh scattering which may cause the weekly reflected light oscillating and amplified between two pumping points (in the case of bidirectional pumping) since our primary focus is to model the entire fiber optic link; instead, we focused only on the dominant effects such as gain and ASE. This is similar to our EDFA modeling which includes only gain and ASE.

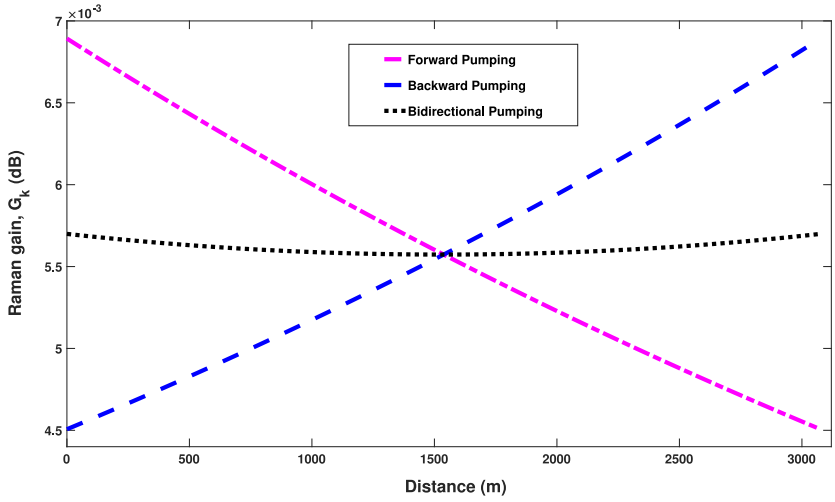

Fig. 6. Gain evolution over the length of the DCF due to Raman amplification. For bidirectional pumping, $\zeta = 1$. Number of Raman tiny amplifires, $N_R = 2000$, total Raman gain = 11.23 dB and length of the DCF = 3.077 km.

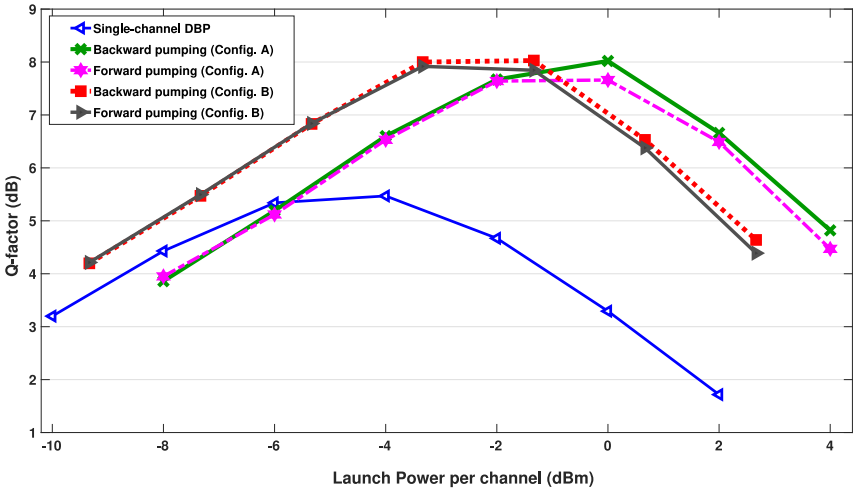

Fig. 7. Q-factor vs. transmitter output power per channel for different schemes when transmission distance is 1500 km.

The signal propagation in fiber is modeled by Manakov equation [43]. The well-known split-step Fourier techniques [1], [6] is used to solve Manakov equation.

To compare the performance of the schemes discussed in Section 3, we study the performance in terms of Q-factor. The Q-factor is calculated using [6],

$$Q = 20 \log_{10} \left[\sqrt{2} erfcinv(2 \times BER) \right], \tag{59}$$

where the BER is the bit error rate computed by the error counting. We compute the mean BER of 10 statistical runs of the fiber optic system and use it in Eq. (59) to calculate the Q-factor. Fig. 7 shows the Q-factor of the central channel as a function of transmitter output power when the transmission distance is 1500 km. At low powers, configuration B shows performance advantage over configuration A which can be attributed to higher OSNR. We can also see that both forward and backward pumping schemes show almost the same performance in the linear region which is due

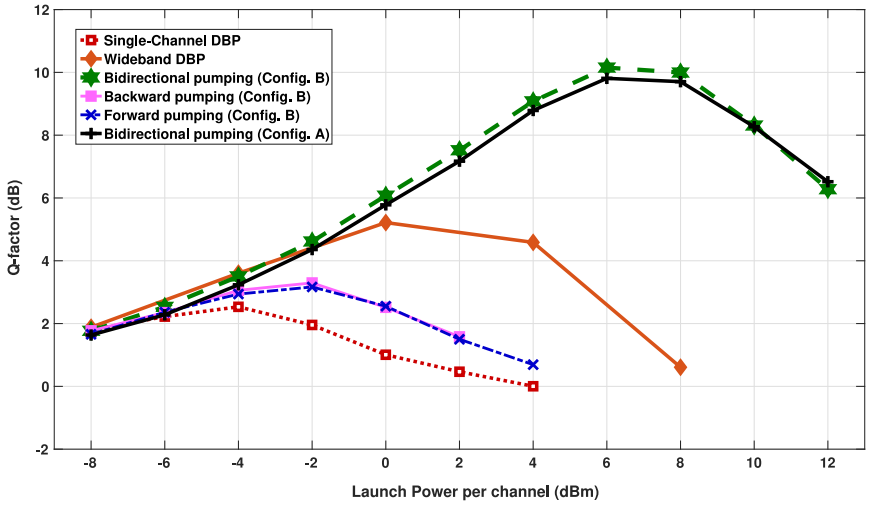

Fig. 8. Q-factor vs. launch power to the TF per channel for different schemes when transmission distance is 5000 km.

to the fact that for a short length of Raman pumped fiber, overall noise figure is almost the same for both pumping schemes, although for a longer length of the fiber, overall noise figure depends on the pumping scheme [44]. From Fig. (7), it can be seen that for both configurations, backward pumping has a sligthly better performance than forward pumping in the nonlinear region ($\geq$0 dBm). This can be explained as follows. The compensation of the nonlinear distoritions caused at the beginning of the transmission fiber span ($z \approxeq 0$) is more important than at the end of the span ($z \approxeq L_a$) since the power is higher at the beginning. The end section of the DCF ($z_d \approxeq L_d$) is responsible for the compensation of the nonlinear distortions occurring at the beginning of the TF ($z \approxeq 0$). As shown in Fig. 4, the signal power for the case of forward pumping is higher than the required power (as required by the ideal OBP condition) at the end section ($z_d \approxeq L_d$) and hence, it introduces more nonlinearity which leads to performance degradation as compared to backward pumping scheme. Both configurations provide roughly 2.5 dB Q-factor gain compared to single-channel DBP. At this distance, we find that the BER of a system with bidirectional pumping for a launch power of 2 dBm and above is below the detection limit; hence, we extend the reach further to be able to compare its performance with other compensation techniques. Fig. 8 shows the Q-factor of the central channel as a function of launch power to the TF when the transmission distance is 5000 km. In the case of single channel DBP, the central channel is demultiplexed at the receiver and the DBP is applied only to the central channel whereas in the case of wideband DBP, full field DBP [45] is applied to all the channels and after the DBP, the central channel is demultiplexed. At the lower launch powers (-8 to -4 dBm), the OBP and DBP schemes provide roughly the same performance since nonlinear impairments are not significant. However, as the launch power increases, the performance of forward/backward pumping schemes gets worse as compared to that of bidirectional Raman pumping scheme. This is because of the second and third order terms in z_d in Eq. (37) which makes the effective loss/gain coefficient α_d to deviate from the ideal OBP condition of Eq. (26). However, using the bidirectional pumping scheme, the performance can be significantly improved. From Fig. 8, we see that the configuration B brings 0.4 dB advantage in Q-factor as compared to the configuration A using bidirectional pumping at the optimum launch power. Using configuration B, the bidirectional pumping scheme (with ratio $\zeta = 1$) provides 6.8 dB improvement in Q-factor as compared to forward/backward pumping scheme. This significant improvement is attributed to the fact that the power profile in the bidirectional pumping scheme is close to the power profile required by the ideal OBP condition. The penalty due to RIN transfer from forward/bidirectional pumping can be neglected due to the high walkoff between pump and signal wavelength in the

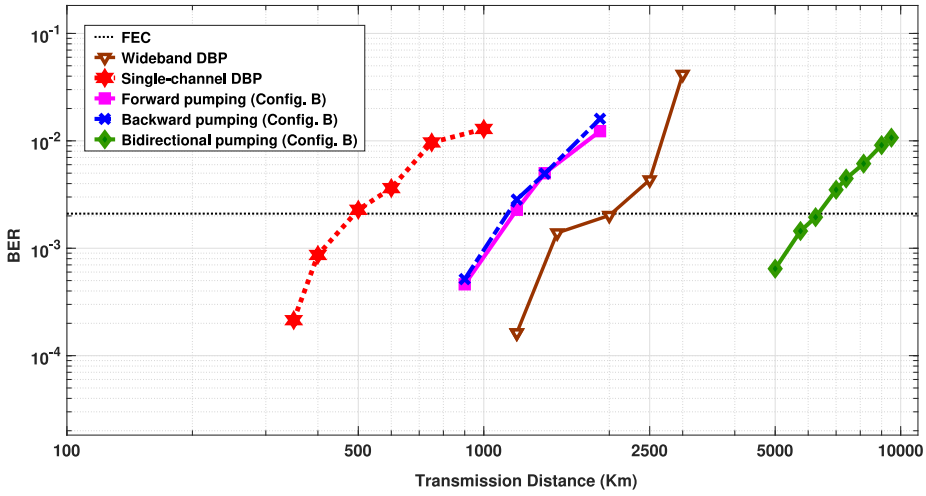

Fig. 9. BER vs. transmission distance.

DCF [46]. As compared to single-channel DBP, OBP based on forward/backward pumping provides a performance advantage of 0.8 dB in Q-factor. At this distance, the wideband DBP has 2 dB performance advantage over OBP based forward/backward pumping scheme. However, wideband DBP requires extensive computational resources and there are technical challenges to combine the outputs of coherent receivers corresponding to different channels. Hence, wideband DBP is not implemented in real time in practical systems. Besides, although in principle, wideband DBP can be used in point-to-point systems, it cannot be implemented in optical networks [31]. In contrast, the OBP schemes provide performance improvements in both point-to-point systems and optical networks. From Fig. 8, we see that the OBP scheme with bidirectional Raman pumping provides 5 dB performance improvement over wideband DBP. This can be explained as follows. Although the wideband DBP compensates for deterministic (signal-dependent) nonlinear impairments, it cannot compensate for stochastic signal-ASE nonlinear impairments such as Gordon-Mollenauer phase noise [7]. However, the OBP scheme with bidirectional Raman pumping provides partial compensation of stochastic signal-ASE nonlinear interactions, since the OPC partially compensates for nonlinear phase noise [47], [48]. Fig. 9 shows the minimum BER as a function of transmission distance. The minimum BER is obtained by optimizing the launch power for each distance. At the BER of 2.1×10^{-3}, the transmission reach of single-channel DBP is about 500 km. OBP based forward/backward pumping scheme enhances the reach to 1150 km. The maximum achievable reach is further extended to 2000 km and 6500 km using wideband DBP and OBP based on bidirectional pumping, respectively.

6. Conclusion

We have investigated an optical back propagation technique to compensate for the dispersion and nonlinearity of the transmission fibers in real time. We have identified the conditions under which the nonlinear effects (both intra- and inter-channel nonlinearities) can be fully compensated and obtained an analytical expression for the power profile of the signal propagating in Raman pumped DCF which provides the exact compensation of intra- and inter-channel signal-signal nonlinear impairments. Two possible configurations to implement the OBP are introduced and compared. We have studied a WDM system with 64-QAM format and showed that for 1500 km transmission distance, OBP based forward/backward Raman scheme brings 2.45 dB Q-factor gain as compared to single-channel DBP. However, wideband DBP (which compensates for all WDM channels) outperforms the OBP based on forward/backward pumping. This is because of the signal

power profile in the DCF deviates from the ideal OBP condition due to the pump loss. Therefore, we proposed a third OBP scheme based on bidirectional pumping. We found that the signal power profile deviation from the ideal OBP profile is minimum when the forward and backward pump power are equal. Using this optimized pump powers, OBP based on bidirectional pumping outperforms that with forward/backward pumping. For 5000 km transmission distance, the performance of the proposed OBP schemes are compared with wideband DBP and single-channel DBP. Bidirectional pumping provides 5 dB performance advantage over wideband DBP. This is due to the fact that the OBP can also provide partial compensation for stochastic nonlinear impairments whereas wideband DBP despite its high complexity cannot. Simulation results show that the transmission reach can be enhanced roughly by a factor of 2.4 using the OBP based on forward/backward pumping and by a factor of 13 using the OBP based on bidirectional pumping, as compared to single-channel DBP.

References

[1] G. P. Agrawal, *Nonlinear Fiber Optics*, 5th ed. New York, NY, USA: Academic, 2012.
[2] R. Essiambre, B. Mikkelsen, and G. Raybon, "Intra-channel cross-phase modulation and four-wave mixing in high-speed TDM systems," *Electron. Lett.*, vol. 35, no. 18, pp. 1576–1578, Sep. 1999.
[3] A. Mecozzi, C. B. Clausen, and M. Shtaif, "System impact of intra-channel nonlinear effects in highly dispersed optical pulse transmission," *IEEE Photon. Technol. Lett.*, vol. 12, no. 12, pp. 1633–1635, Dec. 2000.
[4] S. Kumar, "Intrachannel four-wave mixing in dispersion managed RZ systems," *IEEE Photon. Technol. Lett.*, vol. 13, no. 8, pp. 800–802, Aug. 2001.
[5] P. Poggiolini, "The GN model of non-linear propagation in uncompensated coherent optical systems," *J. Lightw. Technol.*, vol. 30, no. 24, pp. 3857–3879, Dec. 2012.
[6] S. Kumar and M. J. Deen, *Fiber Optic Communications: Fundamentals and Applications*. Hoboken, NJ, USA: Wiley, May 2014.
[7] J. P. Gordon and L. F. Mollenauer, "Phase noise in photonic communications systems using linear amplifiers," *Opt. Lett.*, vol. 15, no. 23, pp. 1351–1353, Dec. 1990.
[8] S. Kumar, "Effect of dispersion on nonlinear phase noise in optical transmission systems," *Opt. Lett.*, vol. 30, no. 24, pp. 3278–3280, Dec. 2005.
[9] A. Mecozzi, "Limits to long-haul coherent transmission set by the Kerr nonlinearity and noise of the in-line amplifiers," *J. Lightw. Technol.*, vol. 12, no. 11, pp. 1993–2000, Nov. 1994.
[10] R. J. Essiambre and P. J. Winzer, "Fibre nonlinearities in electronically pre-distorted transmission," in *Proc. 31st Eur. Conf. Opt. Commun.*, Sep. 2005, vol. 2, pp. 191–192.
[11] K. Roberts, C. Li, L. Strawczynski, M. O'Sullivan, and I. Hardcastle, "Electronic precompensation of optical nonlinearity," *IEEE Photon. Technol. Lett.*, vol. 18, no. 2, pp. 403–405, Jan. 2006.
[12] E. Ip and J. M. Kahn, "Compensation of dispersion and nonlinear impairments using digital backpropagation," *J. Lightw. Technol.*, vol. 26, no. 20, pp. 3416–3425, Oct. 2008.
[13] X. Li *et al.*, "Electronic post-compensation of WDM transmission impairments using coherent detection and digital signal processing," *Opt. Exp.*, vol. 16, no. 2, pp. 880–888, 2008.
[14] E. Mateo, L. Zhu, and G. Li, "Impact of XPM and FWM on the digital implementation of impairment compensation for WDM transmission using backward propagation," *Opt. Exp.*, vol. 16, no. 20, pp. 16124–16137, 2008.
[15] L. B. Du and A. J. Lowery, "Improved single channel backpropagation for intra-channel fiber nonlinearity compensation in long-haul optical communication systems," *Opt. Exp.*, vol. 18, no. 16, pp. 17075–17088, 2010.
[16] Z. Tao, L. Dou, W. Yan, L. Li, T. Hoshida, and J. C. Rasmussen, "Multiplier-free intrachannel nonlinearity compensating algorithm operating at symbol rate," *J. Lightw. Technol.*, vol. 29, no. 17, pp. 2570–2576, 2011.
[17] J. Shao, S. Kumar, and X. Liang, "Digital back propagation with optimal step size for polarization multiplexed transmission," *IEEE Photon. Technol. Lett.*, vol. 25, no. 23, pp. 2327–2330, Dec. 2013.
[18] T. Oyama *et al.*, "Robust and efficient receiver-side compensation method for intra-channel nonlinear effects," in *Proc. Opt. Fiber Commun. Conf.*, Mar. 2014, pp. 1–3.
[19] Y. Fan, L. Dou, Z. Tao, T. Hoshida, and J. C. Rasmussen, "A high performance nonlinear compensation algorithm with reduced complexity based on XPM model," in *Proc. Opt. Fiber Commun. Conf.*, 2014, pp. 1–3.
[20] Y. Gao *et al.*, "Simplified nonlinearity pre-compensation using a modified summation criteria and non-uniform power profile," in *Proc. Opt. Fiber Commun. Conf.*, Mar. 2014, pp. 1–3.
[21] X. Liang and S. Kumar, "Multi-stage perturbation theory for compensating intra-channel nonlinear impairments in fiber-optic links," *Opt. Exp.*, vol. 22, no. 24, pp. 29733–29745, 2014.
[22] X. Liang, S. Kumar, J. Shao, M. Malekiha, and D. V. Plant, "Digital compensation of cross-phase modulation distortions using perturbation technique for dispersion-managed fiber-optic systems," *Opt. Exp.*, vol. 22, no. 17, pp. 20634–20645, 2014.
[23] X. Liang and S. Kumar, "Correlated digital back propagation based on perturbation theory," *Opt. Exp.*, vol. 23, no. 11, pp. 14655–14665, 2015.
[24] D. Pepper and A. Yariv, "Compensation for phase distortions in nonlinear media by phase conjugation," *Opt. Lett.*, vol. 5, no. 2, pp. 59–60, 1980.
[25] S. Watanabe and M. Shirasaki, "Exact compensation for both chromatic dispersion and Kerr effect in a transmission fiber using optical phase conjugation," *J. Lightw. Technol.*, vol. 14, no. 3, pp. 243–248, Mar. 1996.

[26] P. Minzioni *et al.*, "Experimental demonstration of nonlinearity and dispersion compensation in an embedded link by optical phase conjugation," *IEEE Photon. Technol. Lett.*, vol. 18, no. 9, pp. 995–997, May 2006.
[27] M. Morshed, L. B. Du, B. Foo, M. D. Pelusi, and A. J. Lowery, "Optical phase conjugation for nonlinearity compensation of 1.21-tb/s Pol-Mux coherent optical OFDM," in *Proc. 18th Opto Electronics Commun. Conf.*, 2013, Paper PD3-4.
[28] M. D. Pelusi, "WDM signal all-optical pre-compensation of the fiber nonlinearity in dispersion-managed links," *IEEE Photon. Technol. Lett.*, vol. 25, no. 1, pp. 71–74, Jan. 2013.
[29] K. Solis-Trapala, T. Inoue, and S. Namiki, "Nearly-ideal optical phase conjugation based nonlinear compensation system," in *Proc. Opt. Fiber Commun. Conf.*, Mar. 2014, pp. 1–3.
[30] X. Liang, S. Kumar, and J. Shao, "Ideal optical backpropagation of scalar NLSE using dispersion-decreasing fibers for WDM transmission," *Opt. Exp.*, vol. 21, no. 23, pp. 28668–28675, Nov. 2013.
[31] X. Liang and S. Kumar, "Optical back propagation for compensating nonlinear impairments in fiber optic links with ROADMs," *Opt. Exp.*, vol. 24, no. 20, pp. 22682–22692, Oct. 2016.
[32] X. Liang and S. Kumar, "Optical back propagation for fiber optic networks with hybrid EDFA Raman amplification," *Opt. Exp.*, vol. 25, no. 5, pp. 5031–5043, Mar. 2017.
[33] B. Foo, B. Corcoran, C. Zhu, and A. J. Lowery, "Distributed nonlinear compensation of dual-polarization signals using optoelectronics," *IEEE Photon. Technol. Lett.*, vol. 28, no. 20, pp. 2141–2144, Oct. 2016.
[34] B. Foo, B. Corcoran, and A. J. Lowery, "Distributed nonlinear compensation using optoelectronic circuits," *J. Lightw. Technol.*, vol. 36, no. 6, pp. 1326–1339, Mar. 2018.
[35] P. B. Hansen, G. Jacobovitz-Veselka, L. Gruner-Nielsen, and A. J. Stentz, "Raman amplification for loss compensation in dispersion compensating fibre modules," *Electron. Lett.*, vol. 34, no. 11, pp. 1136–1137, May 1998.
[36] Y. Emori, Y. Akasaka, and S. Namiki, "Broadband lossless DCF using Raman amplification pumped by multichannel WDM laser diodes," *Electron. Lett.*, vol. 34, no. 22, pp. 2145–2146, Oct. 1998.
[37] M. Vasilyev, B. Szalabofka, S. Tsuda, J. M. Grochocinski, and A. F. Evans, "Reduction of Raman MPI and noise figure in dispersion-managed fibre," *Electron. Lett.*, vol. 38, no. 6, pp. 271–272, Mar. 2002.
[38] J. W. Nicholson, "Dispersion compensating Raman amplifiers with pump reflectors for increased efficiency," *J. Lightw. Technol.*, vol. 21, no. 8, pp. 1758–1762, Aug. 2003.
[39] T. J. Xia *et al.*, "Transmission of 400G pm-16 QAM channels over long-haul distance with commercial all-distributed Raman amplification system and aged standard SMF in field," in *Proc. Opt. Fiber Commun. Conf.*, Mar. 2014, pp. 1–3.
[40] M. A. Iqbal, M. Tan, and P. Harper, "On the mitigation of RIN transfer and transmission performance improvement in bidirectional distributed Raman amplifiers," *J. Lightw. Technol.*, vol. 36, no. 13, pp. 2611–2618, Jul. 2018.
[41] H. M. Wang, W. T. Shih, and H. Taga, "Single fiber based 10.66 gb/s bidirectional long reach WDM-PON supported by distributed Raman amplifier," in *Proc. Joint Conf. Opto-Electron. Commun. Conf. Australian Conf. Opt. Fibre Technol.*, Jul. 2008, pp. 1–2.
[42] S. Namiki, N. Tsukiji, and Y. Emori, *Pump Laser Diodes and WDM Pumping*, M. N. Islam, Ed. New York, NY, USA: Springer, 2004.
[43] P. K. A. Wai and C. R. Menyak, "Polarization mode dispersion, decorrelation, and diffusion in optical fibers with randomly varying birefringence," *J. Lightw. Technol.*, vol. 14, no. 2, pp. 148–157, Feb. 1996.
[44] G. M. Isoe, K. M. Muguro, and D. W. Waswa, "Noise figure analysis of distributed fibre Raman amplifier," *J. Sci. Technol. Res.*, vol. 2, no. 11, pp. 375–378, 2013.
[45] X. Li *et al.*, "Electronic post-compensation of WDM transmission impairments using coherent detection and digital signal processing," *Opt. Exp.*, vol. 16, no. 2, pp. 880–888, Jan. 2008.
[46] C. R. S. Fludger, V. Handerek, and R. J. Mears, "Pump to signal RIN transfer in Raman fiber amplifiers," *J. Lightw. Technol.*, vol. 19, no. 8, pp. 1140–1148, Aug. 2001.
[47] S. Kumar and L. Liu, "Reduction of nonlinear phase noise using optical phase conjugation in quasi-linear optical transmission systems," *Opt. Exp.*, vol. 15, no. 5, pp. 2166–2177, Mar. 2007.
[48] S. Rahbarfam and S. Kumar, "Nonlinear phase noise reduction using digital back propagation and midpoint optical phase conjugation," *Opt. Exp.*, vol. 27, no. 6, pp. 8968–8982, Mar. 2019.